CrossMark

# Lateral performance of a semi-rigid timber frame structure: theoretical analysis and experimental study

Yingyang Liu[1] [iD] · Haibei Xiong[2]

## Abstract
Semi-rigidness of the joint connections is one of the main characteristics of timber structures. The pin-joint assumption for the semi-rigid joint connections might be not conservative in the timber structural design. In this paper, structural analysis was conducted on a semi-rigid timber portal frame; the formulas were derived in terms of the internal force and the lateral stiffness, and the influence of the semi-rigid connections was discussed. Moreover, experimental tests were performed on three full-scale timber portal frames and five bolted timber connections to study the lateral performance of the frames and the moment resistance of the connections. For consistency, the connections from the portal frames and the connections for bending tests were of the same configuration. Finally, a calculation flowchart of the lateral performance on a semi-rigid frame was presented to verify the derived formulas and to show a framework of the lateral structural design process.

**Keywords** Semi-rigid connection · Timber frame structure · Lateral performance · Theoretical analysis · Experimental study

## Introduction

The component members of modern heavy timber frames are usually connected with metal connectors, especially via bolted connections with slotted steel plates (Fig. 1) because of the simplicity of these items. Compared with the traditional mortise-and-tenon connection, such connections have more stable performance and better moment resistance. However, it is still difficult to make the bolted connection fully rigid [1–3]. To address this issue, the current design methodology generally ignores its capacity of carrying moments and uses the pin-joint assumption.

However, the pin-joint assumption also has drawbacks. In reality, such connections can experience bending moments, which are not considered in the design and cause longitudinal shear and tension perpendicular to the grain in timber. The connection can be prone to a premature brittle failure

when the timber frame is subjected to a lateral force, particularly that induced by an earthquake.

Lam et al. [4] conducted experimental studies on the moment resistance of bolted timber connections. A total of 30 connection tests were conducted, including specimens with regular connections and connections reinforced with self-tapping screws. The test results showed that the bolted timber connections were able to carry moment load, and the application of the self-tapping screws could improve the ductility of the connection. Kasal et al. [5] reinforced beam-to-column connections using self-tapping screws and used hardwood blocks to support the beams. The study aimed to seek a solution of a rigid timber joint connection. The results showed that the rigid connection worked well, and a highly linear moment-resisting behavior was observed. However, the exceedingly linear behavior of the connection could cause a brittle failure of the frame. Kohara [6], Komatsu et al. [7], and Noguchi et al. [8] conducted reverse cyclic loading tests on the portal frames to study the lateral strength and their ductility. Those results showed that the timber portal frames had excellent deformability but with inadequate lateral stiffness. Lateral reinforcements for the timber frame then drew the attention of academic scholars [9–11].

The studies above indicate that the bolted timber connection can carry moment load and that the bolted timber frame

✉  Yingyang Liu
    liuyingyang5687@qq.com

1   School of Civil Engineering, Zhengzhou University, No. 100 Science Avenue, Zhengzhou 450001, China

2   College of Civil Engineering, Tongji University, No. 1239 Siping Road, Shanghai 200092, China

**Fig. 1** Bolted timber connection with a slotted steel plate

can also resist lateral load. To study the relationship between the semi-rigid connection and the lateral performance of the semi-rigid frame, Shu [12] and Duan [13] adopted nonlinear rotational springs and applied them for the semi-rigid connection in a finite-element model. The structural response was calculated step by step; however, the implicit numerical solution was not very conducive to the qualitative analysis of the factors affecting the lateral performance of the structure. Zonta [14] and Wang [15] assumed the semi-rigid frame as a rigid frame or a partly rigid frame to obtain the structural internal force from the classic method of the structural mechanics and then to obtain an analytical solution by superposition of the rotations of the semi-rigid joints. However, these analytical solutions were not accurate, because the semi-rigid joints affect the internal force distribution of the structure.

In this paper, a theoretical analysis on the semi-rigid frame was conducted, considering all of the connections following the semi-rigid assumption, and analytical formulas were derived. Next, experimental studies were conducted on three bolted timber frames and five bolted timber connections with the same configuration as that of the frames. Finally, a calculation flowchart of the lateral performance on a semi-rigid frame was presented; the theoretical calculation on the timber frame and the test result was compared to verify the derived formulas.

## Structural analysis on the semi-rigid frame

While the theory developed in this paper is completely general, only a one-story, one-bay portal frame is studied in detail. This portal frame has semi-rigid connections at the intersection of

the members and is subjected to a horizontal lateral load $F$, as shown in Fig. 2. Note that $E$ is the modulus of the timber member; $K$ is the bending stiffness of the joint; $H$, $L$, and $I$ are the geometric parameters of structure representing the height of the column, the length of the beam and the moment of inertia of the member section, respectively; $M$ is the internal moment load; and subscripts "c" and "b" are for column and beam.

The column (Fig. 3) is considered an Euler beam, and the curvature is thus expressed as

$$w''(y) = \frac{M(y)}{E_c I_c} = \frac{1}{E_c I_c}\left(M_b - \frac{F}{2}H + \frac{F}{2}y\right). \tag{1}$$

The rotation $\theta(y)$ and the deflection $w(y)$ of the column are, therefore

$$\theta(y) = \frac{1}{E_c I_c}\left[\left(M_b - \frac{F}{2}H\right)y + \frac{F}{4}y^2\right] + A_1 \tag{2}$$

$$w(y) = \frac{1}{E_c I_c}\left[\frac{1}{2}\left(M_b - \frac{F}{2}H\right)y^2 + \frac{F}{12}y^3\right] + A_1 y + A_2 \tag{3}$$
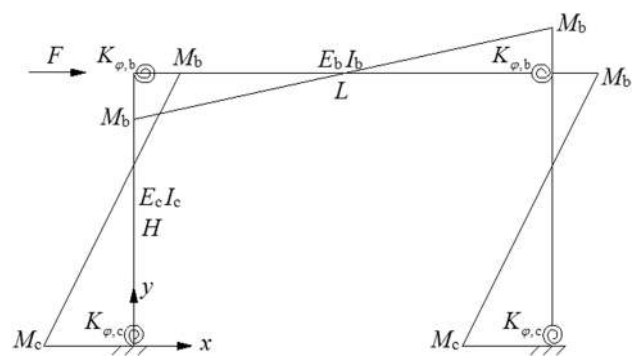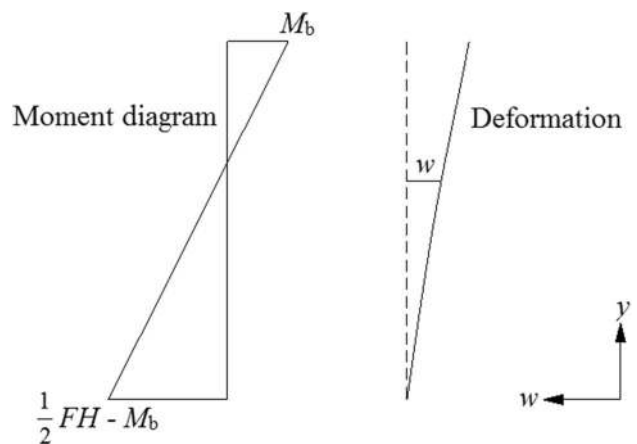


**Fig. 2** Mechanical model of the semi-rigid frame



**Fig. 3** Free-body diagram of the column

where $A_1$ and $A_2$ are integration constants. At the bottom of the column ($y = 0$), the rotation is $\theta(0) = \frac{1}{K_{\varphi,c}}\left(M_b - \frac{F}{2}H\right)$, and the deflection is $w(0) = 0$; therefore, the values of $A_1$ and $A_2$ can be calculated as $A_1 = -\frac{1}{K_{\varphi,c}}\left(\frac{F}{2}H - M_b\right)$ and $A_2 = 0$.

The same can be obtained from the beam (Fig. 4). The rotation $\beta(x)$ and the deflection $v(x)$ of the beam are expressed as

$$\beta(x) = \frac{1}{E_b I_b}\left(M_b x - \frac{M_b}{L}x^2\right) - \frac{1}{6}\frac{1}{E_b I_b}M_b L \tag{4}$$

$$v(x) = \frac{1}{E_b I_b}\left(\frac{1}{2}M_b x^2 - \frac{1}{3}\frac{M_b}{L}x^3\right) - \frac{1}{6}\frac{1}{E_b I_b}M_b L x. \tag{5}$$

At the intersection of the column and beam, where $y = H$ and $x = 0$, the compatibility of the rotation is

$$|\theta(H)| = |\beta(0)| + \frac{M_b}{K_{\varphi,b}} \tag{6}$$

or, substituting positive and negative values, is

$$-\theta(H) = -\beta(0) + \frac{M_b}{K_{\varphi,b}}. \tag{7}$$

Introducing Eqs. (2) and (4), the solution of the bending moment is

$$M_b = \frac{\frac{1}{2i_c} + \frac{1}{K_{\varphi,c}}}{\frac{1}{i_c} + \frac{1}{6i_b} + \frac{1}{K_{\varphi,c}} + \frac{1}{K_{\varphi,b}}}\frac{H}{2}F \tag{8}$$

$$M_c = \frac{\frac{1}{2i_c} + \frac{1}{6i_b} + \frac{1}{K_{\varphi,b}}}{\frac{1}{i_c} + \frac{1}{6i_b} + \frac{1}{K_{\varphi,c}} + \frac{1}{K_{\varphi,b}}}\frac{H}{2}F \tag{9}$$

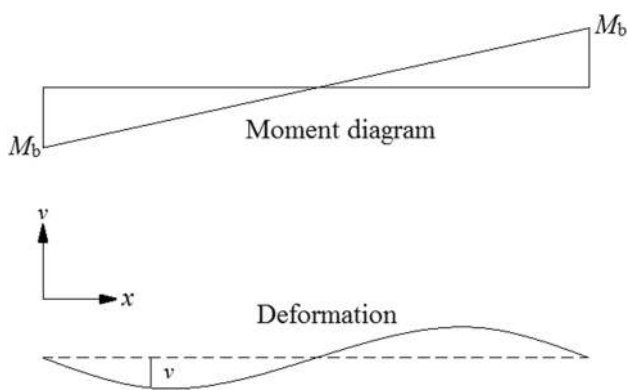where $i_c = \frac{E_c I_c}{H}$ and $i_b = \frac{E_b I_b}{L}$.



**Fig. 4** Free-body diagram of the beam

Therefore, the expressions of the structural displacement and stiffness are

$$\Delta = \frac{\frac{1}{i_c}\left(\frac{1}{12i_c} + \frac{1}{18i_b} + \frac{1}{3K_{\varphi,c}} + \frac{1}{3K_{\varphi,b}}\right) + \frac{1}{K_{\varphi,c}}\left(\frac{1}{6i_b} + \frac{1}{K_{\varphi,b}}\right)}{\frac{1}{i_c} + \frac{1}{6i_b} + \frac{1}{K_{\varphi,c}} + \frac{1}{K_{\varphi,b}}}\frac{H^2}{2}F \tag{10}$$

$$K = \frac{\frac{1}{i_c} + \frac{1}{6i_b} + \frac{1}{K_{\varphi,c}} + \frac{1}{K_{\varphi,b}}}{\frac{1}{i_c}\left(\frac{1}{12i_c} + \frac{1}{18i_b} + \frac{1}{3K_{\varphi,c}} + \frac{1}{3K_{\varphi,b}}\right) + \frac{1}{K_{\varphi,c}}\left(\frac{1}{6i_b} + \frac{1}{K_{\varphi,b}}\right)} \cdot \frac{2}{H^2} = \eta \cdot \frac{i_c}{H^2} \tag{11}$$

where $\eta = \frac{12(6+\alpha+6\gamma+6\beta\gamma)}{3+2\alpha+12\gamma+6\alpha\gamma+12\beta\gamma+36\beta\gamma^2}$ is a dimensionless design parameter, and $\alpha = \frac{i_c}{i_b}$, $\beta = \frac{K_{\varphi,c}}{K_{\varphi,b}}$, and $\gamma = \frac{i_c}{K_{\varphi,c}}$.

From Eqs. (10) and (11), it can be concluded that the bending stiffness of the connections (namely, the semi-rigidness of the connections) does affect the lateral performance of the frame structure and has a same order effect with the stiffness of the beam and column. If a design is conducted reasonably, then the semi-rigid frame can effectively resist the lateral load. The simplified Eq. (11) can be used practically in the design.

Furthermore, when $K_{\varphi,c} \to \infty$ and $K_{\varphi,b} \to \infty$, $M_b = \frac{3i_b}{6i_b+i_c}\frac{H}{2}F$, and $M_c = \frac{3i_b+i_c}{6i_b+i_c}\frac{H}{2}F$; when $K_{\varphi,c} \to 0$ and $K_{\varphi,b} \to \infty$, $M_b = \frac{H}{2}F$ and $M_c = 0$; and when $K_{\varphi,c} \to \infty$ and $K_{\varphi,b} \to 0$, $M_b = 0$, and $M_c = \frac{H}{2}F$. All of the above are consistent with the calculations from the structural mechanics.

## Experimental study on the lateral performance of bolted timber frames

### Specimen design

Three full-scale, one-story, one-bay timber post, and beam construction specimens were designed for the experimental study. All of the specimens had a span of 4110 mm and a height of 2740 mm (span–depth ratio of 1.5). The column sections were 280 mm × 230 mm, and the beam sections were 280 mm × 180 mm. The joint connections were bolted glulam connections slotted in steel plates. The layouts of the specimens [16] are shown in Fig. 5.

Canadian spruce-pine-fir (SPF) glued-laminated timber was used to fabricate the columns and beams; the wood mechanical properties are listed in Table 1. Bolts with a grade of 8.8 (equivalent to ASTM A325 bolts), conforming to Chinese Standard GB\T1231-2006 [17], were used as the fasteners of the specimens. The maximum tensile strength of the bolts was 800 MPa, and the yield point of the bolts was 640 MPa. Mild carbon steel Q235B with a thickness of 10 mm, conforming to Chinese Standard GB 50017-2003
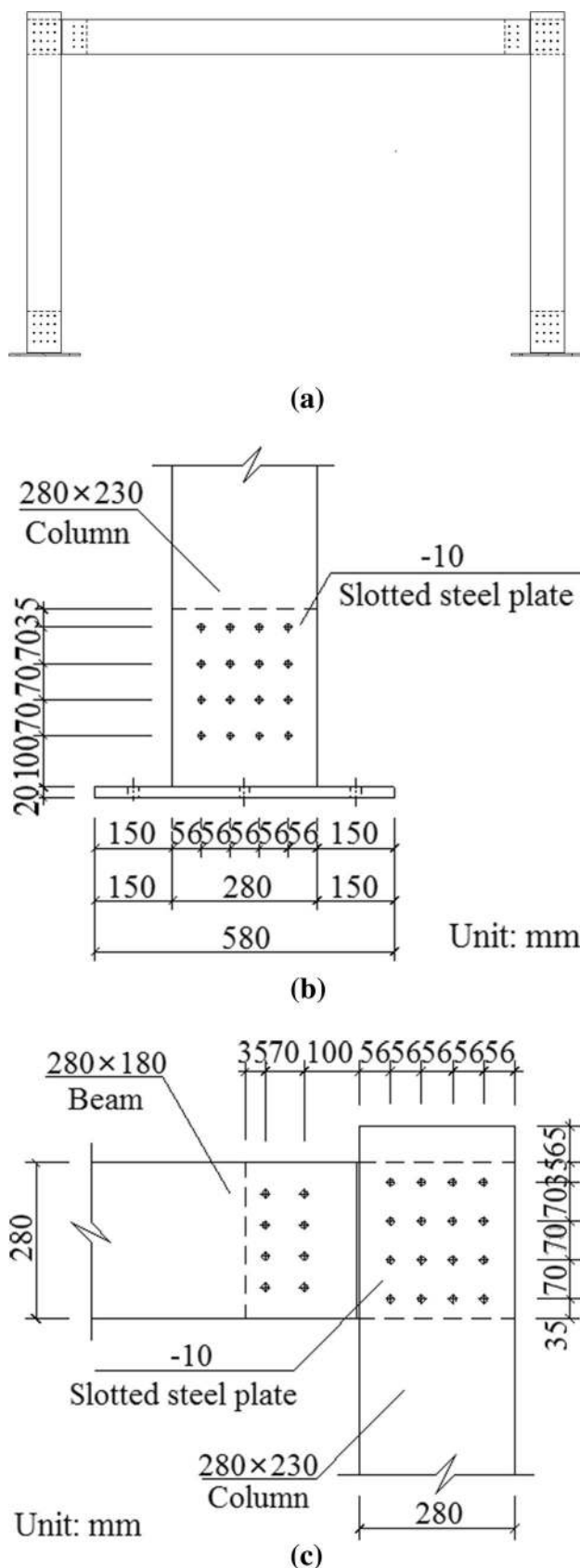
Fig. 5 Layouts of the timber frame. **a** Sketch of the bolted timber frame. **b** Column-bottom joint. **c** Beam-to-column joint

[18], was used as steel plates for the connections. The yield point of the steel plates was 235 MPa; a steel plate was used for one joint connection only, without reuse. The moisture content of the specimens ranged from 12 to 14% during the tests.

## Test setup and procedure

Experimental tests were conducted using a hydraulic actuator (Schenker hydraulic loading system manufactured by American MTS Systems Corporation) at Tongji University. The hydraulic actuator had a displacement range of ± 250 mm and a capacity of 650 kN. The actuator was secured between the concrete reaction wall and the steel plate at the elevation corresponding to the top of the column. There was a hinge between the hydraulic actuator and the steel plate to eliminate the bending moment generated by the gravity of the actuator so that the horizontal reverse load could be applied more simply. The pulling load was transferred by the steel tie bar to avoid the partial failure of the left beam–column joint. For the boundary conditions, the bottom of the columns was fixed by eight bolts (22-mm diameters) to the ground beam. The out-of-plane stability was ensured via a steel roller installed on the gantries. Figures 6 and 7 show the test setup and instrumentation, respectively.

One specimen was tested monotonically, and the other two were loaded cyclically. The horizontal load was applied using a displacement control method, and the cyclic test procedure referred to the Method B of the American Society for Testing and Materials (ASTM) E2126 [19]. The test was terminated either when the load decreased to 80% of the ultimate load or when the lateral displacement reached 250 mm.

## Experimental phenomenon and failure mode

The joints were examined for local pressing (Fig. 8) as the lateral displacement increased. The bottom of the columns first split when the lateral displacement reached 50 mm (1.8% drift ratio); cleavage cracks then occurred at the end of the beams at a lateral displacement of approximately 100 mm (3.6% drift ratio). The cleavage cracks continued to develop (Fig. 9) during the subsequent loading process without significant load reduction. The test was terminated when the lateral displacement reached 250 mm (9.1% drift ratio).

The failure mode of the simple frame indicated that the joints were weak but that the members were strong. When the simple frame was subjected to lateral loading, the semi-rigid joint connections experienced bending moments, which created tension perpendicular to the wood grain and a longitudinal shear stress (the two weakest strength properties of timber), which likely caused the premature splitting at the joints. Thus, the simple frame with wood–steel–wood-bolted

**Table 1** Wood mechanical properties tested by the authors

| $E_L$ (N/mm²) | $E_P$ (N/mm²) | $\sigma_{L,t}$ (N/mm²) | $\sigma_{L,c}$ (N/mm²) | $\sigma_{P,c}$ (N/mm²) | $\rho$ (kg/m³) |
|---|---|---|---|---|---|
| 9542 | 334 | 46.7 | 26.1 | 3.8 | 467 |

$E$ elastic modulus, $\sigma$ stress strength, $\rho$ density, $L$ longitudinal to wood grain, $P$ perpendicular to wood grain, $t$ tension, $c$ compression.
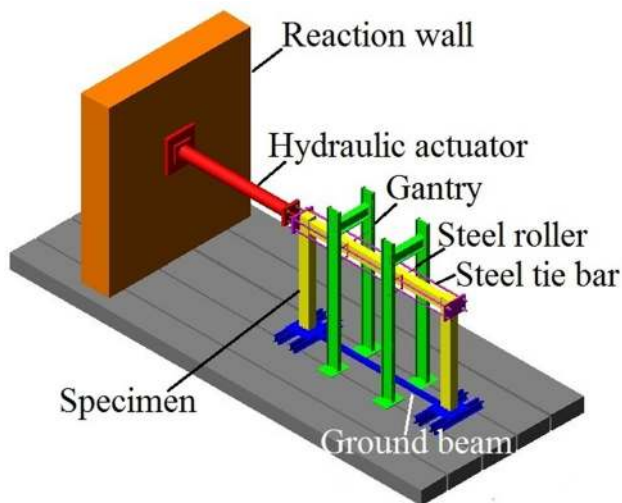


**Fig. 6** Test setup for the timber frame



**Fig. 7** Test instrumentation



**Fig. 8** Local pressing of the frame joints. **a** Column-bottom joint. **b** Beam-to-column joint

joint connections was damaged under lateral loading. Although the simple frame specimen showed premature splitting at the joints, it had a very strong deformation capability without significant load drop or collapse.

## Moment-resisting tests on bolted timber connections

### Test program

To conduct a systematic study on the mechanical mechanism of the semi-rigid frame structure, bolted timber connections with the same materials and configuration as the those in the
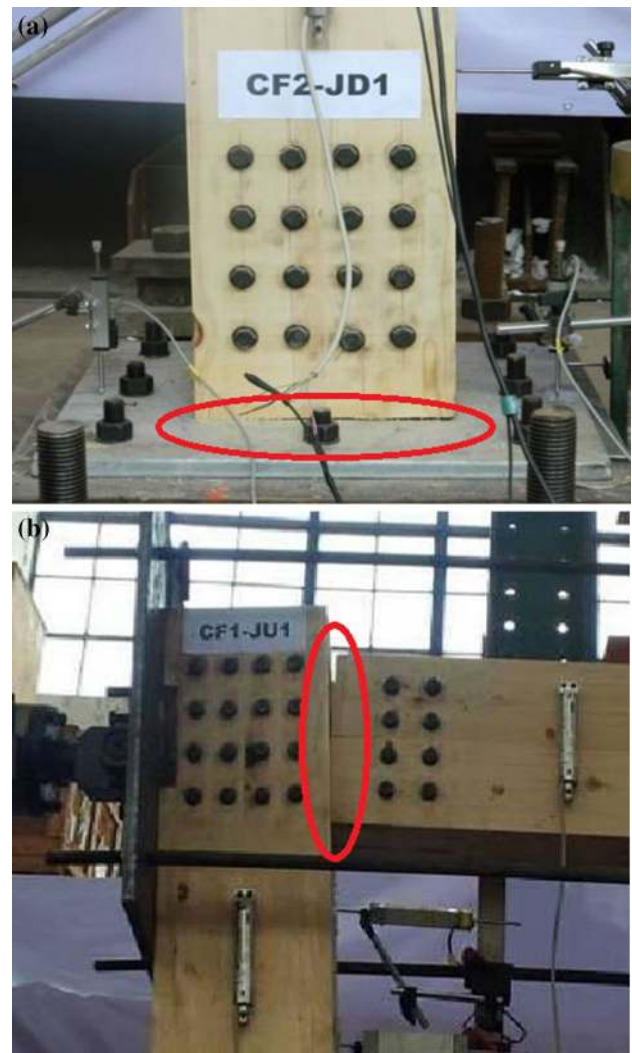
portal frame were tested. Five full-scale replicate specimens were designed in the test program.

The tests were conducted in the timber testing laboratory at Tongji University. Figure 10 illustrates the general setup of the tests [20]. A hydraulic actuator with a displacement range of ± 250 mm and a capacity of 300 kN was used to apply the horizontally reversed load. The connection specimens were rotated 90° for ease of loading. The column member was fixed on the ground using steel anchor bolts. The hydraulic actuator was attached to the top end of the beam member by a rotatable steel cage. Steel blocks were
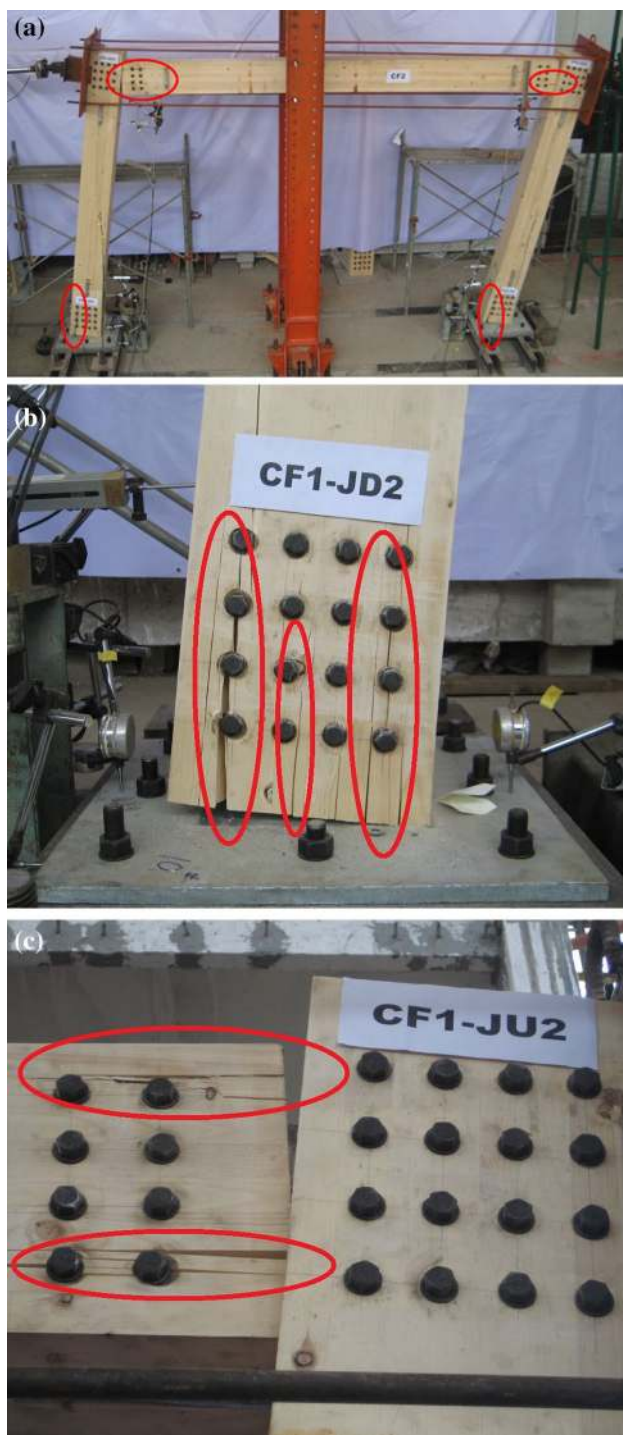
Fig. 9 Failure mode of the bolted timber frame. **a** Bolted timber frame under lateral loading. **b** Column-bottom joint. **c** Beam-to-column joint



**Fig. 10** Test setup for the joint connection

a procedure referring the Consortium of Universities for Research in Earthquake Engineering (CUREE) displacement-controlled cyclic protocol [21]. The actuator recorded both the lateral displacement and the load. The force arm was assumed as the distance from the loading point to the center of the bolts group. Rotation (the lateral displacement divided by the force arm) and moment (the lateral load multiplied by the force arm) were then determined.

## Experimental phenomenon and failure mode

No significant failure was observed in the early loading process of the connections; however, sounds were detected near the wood and bolt contact areas. The wood member split first around the bolts on the tension side of the beam member at the rotation of approximately 6°, and then, the cleavage cracks continued to develop along the wood grain. Crushed timber was also found in the compression area between the column and the beam. Eventually, the specimen failed with (bolt) row shear on the beam (Fig. 11a).

After disassembly (Fig. 11b), the bolts in the beam were observed to experience more bending, whereas the bolts in the column remained nearly straight. Dowel-bearing failure was found in most holes.

## Results and discussion

### Experimental data

Experimental data of the displacement–load curves of the frames and the rotation–moment curves of the connections are shown in Fig. 12. For cyclic tests, the curves in the figure represent the envelope curves. The mechanical performance parameters of the specimens are listed in Table 2.
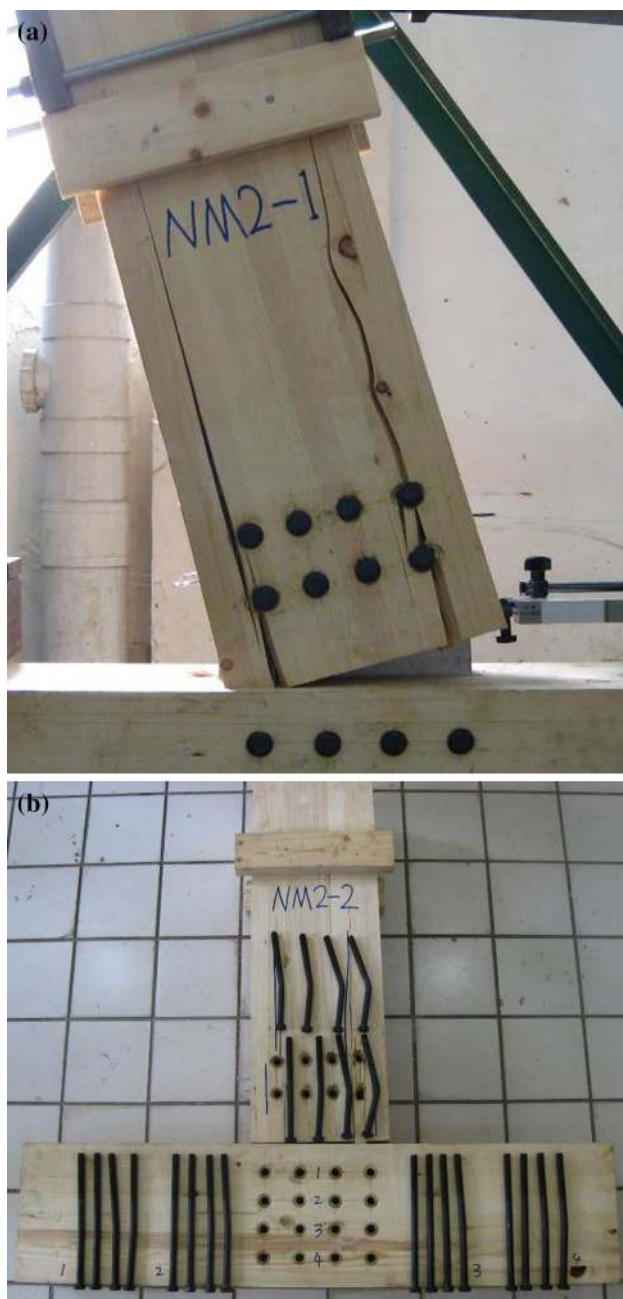
placed in the gaps between the reaction frame and the column member on both sides to restrict horizontal rigid body movement.

Two tests of the specimens were conducted under monotonic loading, and the other three were tested using

**Fig. 11** Failure mode of the bolted joint connection. **a** Row shear failure. **b** Bending of the bolts



**Fig. 12** Experimental data. **a** Displacement–load curves of the frames. **b** Rotation–moment curves of the connections. *M* monotonic test, *C* cyclic test

**Table 2** Mechanical performance parameters of the experimental tests

| Test type | Specimen | $K_e$ | $P_{peak}$ |
|---|---|---|---|
| Frame | M1 | 0.4 kN/mm | 57.5 kN |
| | C1 | 0.3 kN/mm | 54.5 kN |
| | C2 | 0.4 kN/mm | 55.5 kN |
| Connection | M1 | 4.4 kNm/° | 27.9 kNm |
| | M2 | 4.4 kNm/° | 29.1 kNm |
| | M3 | 4.2 kNm/° | 33.7 kNm |
| | C1 | 4.5 kNm/° | 35.3 kNm |
| | C2 | 4.7 kNm/° | 35.6 kNm |

$K_e$ elastic stiffness, $P_{peak}$ load bearing capacity

The bolted timber frames can resist the lateral load effectively, behaving more similar to a structure rather than a geometrically unstable system. The theoretical study in this paper also indicated that the semi-rigid frame can provide a certain lateral resistance related to the bending stiffness of the connections. The bolted timber connections experienced a nonlinear moment bearing process and showed an obvious semi-rigid characteristic. In the next section, the obtained mechanical properties of the connections are used to predict the entire structural response based on the derived formulas.
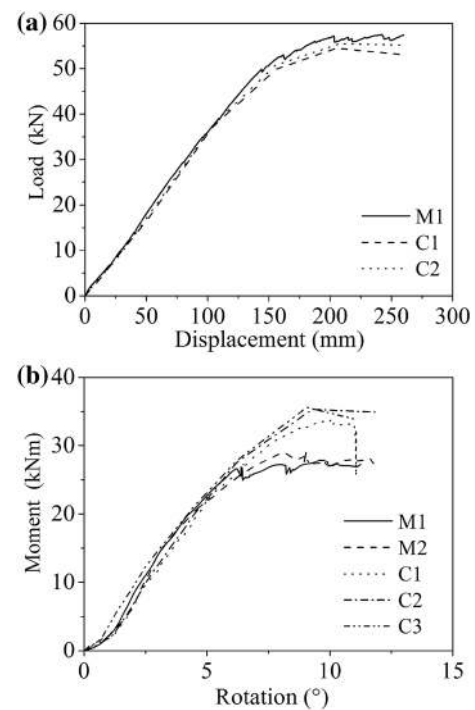
## Theoretical calculation of the structural response of the semi-rigid frame

The structural response of the semi-rigid frame under lateral loading had a corresponding relationship to the mechanical status of the joint connections (Fig. 13). This corresponding relationship could be determined using the derived formulas in this paper. The calculation process is as follows:
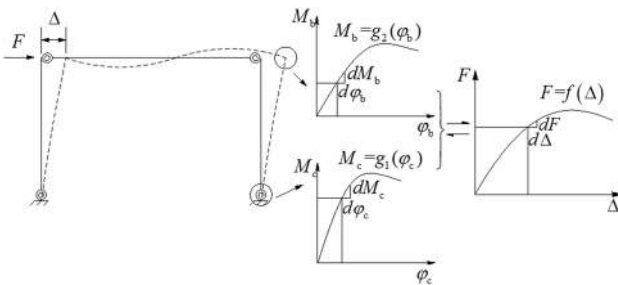
**Fig. 13** Relationship between joint mechanical status and structural lateral displacement



**Fig. 14** Finite-element model of the semi-rigid frame

## Determine the initial state of the structure

The lateral displacement $\Delta_0$, structural force $F_0$, rotation at the column bottom $\varphi_{c,0}$, and rotation at the intersection of the column and beam $\varphi_{b,0}$ were determined initially as 0. Note that other initial values are also applicable.

The rational stiffness of the column-bottom joint and the column-to-beam joint at the initial state, $K_{c,0}$ and $K_{b,0}$, can be obtained from the curve of function $g$ (Fig. 13). In this paper, function $g_2$ for the beam-to-column joint was determined by the average curve of the test data (Fig. 12b); function $g_1$ for column-bottom joint was determined by the result of the numerical simulation [22]. The structural stiffness at the initial state, $K_{s,0}$, can be calculated using Eq. (11).

## Define the basic increment and the unknown

In this paper, the rotation at the column bottom, $d\varphi_c$, was chosen as the basic known increment; the increment of the structural force, $dF$, was taken as the basic unknown.

## Calculate other structural increments

When $d\varphi_c$ is sufficiently small, the moment increment at the column bottom can be determined as

$$dM_c = d\varphi_c \cdot K_{c,0}. \tag{12}$$

Introducing the increment of the structural force, $dF$, the moment increment at the intersection of the column and beam is

$$dM_b = \frac{H}{2}dF - dM_c. \tag{13}$$

The increment of the rotation is still compatible at the column-to-beam joint, and Eq. (7) is applicable here to obtain the solution of the only unknown, $dF$.
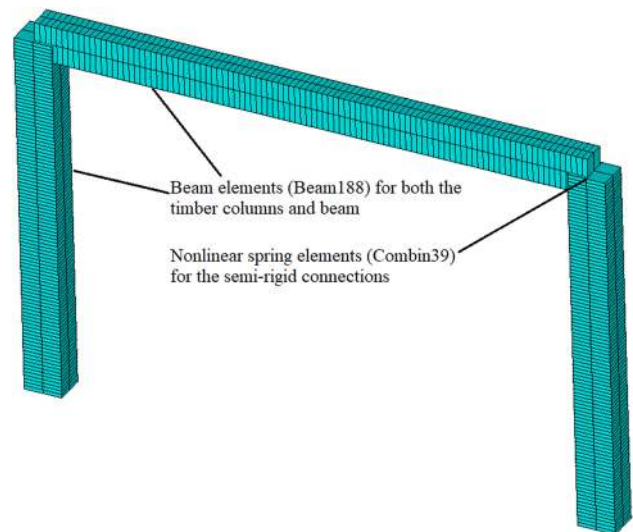
Thus, the rotation increment of the beam-to-column joint is $d\varphi_b = \frac{dM_b}{K_{b,0}}$, and the increment of the lateral displacement is $d\Delta = \frac{dF}{K_{s,0}}$.

## Determine the next state of the structure

After the first structural increment, the next state of the structure is as follows: lateral displacement $\Delta_1 = \Delta_0 + d\Delta$, structural force $F_1 = F_0 + dF$, rotation at the column bottom $\varphi_{c,1} = \varphi_{c,0} + d\varphi_c$ and rotation at the intersection of the column and beam $\varphi_{b,1} = \varphi_{b,0} + d\varphi_b$.

$K_{c,1}$, $K_{b,1}$, and $K_{s,1}$ can be calculated in the same manner.

Cycle through steps 1–4 to obtain the overall structural displacement–force relationship and the corresponding joint status at every cycle. The software MATLAB was adopted to run the cycles.

## Numerical simulation on the semi-rigid frame

To further verify the theoretical calculation, a finite-element (FE) model was established using the commercial finite-element program ANSYS. Structural information was exactly the same as that of the theoretical study. Nonlinear spring elements (Combin39) were adopted to simulate the semi-rigid connections; points on the curve of function $g_1$ and $g_2$ were used to define the spring elements. The timber columns and beam were simulated by the beam elements (Beam188). The FE model is shown in Fig. 14. Lateral loading was applied on the top of the FE model and the force–deformation curve was obtained for the comparison.
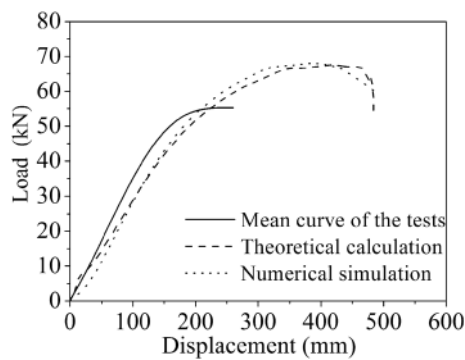
**Fig. 15** Comparison of the test result, theoretical calculation, and numerical simulation

## Comparison of the test result, theoretical calculation, and numerical simulation

Comparison of the test result, theoretical calculation and numerical simulation is shown in Fig. 15. It should be noted that the curve of the test result used the mean curve of the three test curves in Fig. 12a.

The test result and the theoretical calculation were not very consistent. The reason is that in the experimental tests, the rotation centers of the connections varied (due to the members' compression and wood splitting) during the loading process, while in the mechanical model, the connections were simulated by nonlinear spring elements with fixed rotation centers. As a result, the comparison between the two shows some difference in both stiffness and strength. However, overall, the theoretical calculation predicted the load capacity and could be useful to provide the information of the subsequent loading process beyond the experimental limitation.

Comparing the curves of the theoretical calculation and the numerical simulation, these two matched well and the theoretical algorithm was further verified. It could be concluded that once the rotation centers of the frame joint connections were strictly obtained and then implanted in the calculation, the theoretical result could guide the structural design well.

## Conclusions

In this paper, theoretical analysis and an experimental study were conducted on the semi-rigid timber frame structure. Moment-resisting tests on the bolted timber connections showed an obvious semi-rigid characteristic, and the bolted timber frame was found to carry the lateral load well. The frame failed in the splitting joints and showed a strong member and weak-joint mode. Thus, the current widely used pin-joint assumption in the timber structure design is not very conservative and likely results in premature failure at the joint areas. A theoretical analysis on the semi-rigid frame was conducted, considering all of the connections following the semi-rigid assumption, and analytical formulas were derived. Next, based on the theoretical analysis, a method was proposed to calculate the overall structural lateral response. In practical engineering work, an experimental test or a numerical simulation can be conducted first to obtain the semi-rigidness of the joint connections, and the lateral performance of the structure can be predicted using the derived formulas in this paper.

## References

1. Wang MQ, Song XB, Gu XL, Zhang YF, Luo L (2016) Rotational behavior of bolted beam-to-column connections with locally cross-laminated glulam. J Struct Eng 141:04014121
2. He MJ, Zhao Y, Ma RL (2016) Experimental investigation on lateral performance of pre-stressed tube bolted connection with high initial stiffness. Adv Struct Eng 19:762–776
3. He MJ, Liu HF (2015) Comparison of glulam post-to-beam connections reinforced by two different dowel-type fasteners. Constr Build Mater 99:99–108
4. Lam F, Gehloff M, Closen M (2010) Moment-resisting bolted timber connections. Struct Build 163:267–274
5. Kasal B, Guindos P, Polocoser T, Heiduschke A, Urushadze S, Pospisil S (2014) Heavy laminated timber frames with rigid three-dimensional beam-to-column connections. J Perform Constr Facil 28:A4014014
6. Kohara K (2006) A study on experiment and structural design for timber rigid frame. In: Proceedings 2006 world conference on timber engineering, Oregon State University Conference Services, Corvallis, OR, pp 295–302
7. Komatsu K, Hosokawa K, Hattori S (2006) Development of ductile and high-strength semi-rigid portal frame composed of mixed species glulams and h-shaped steel gusset joints. In: Proceedings 2006 world conference on timber engineering, Oregon State Univ. Conference Services, Corvallis, OR, pp 303–310
8. Noguchi M, Takino S, Komatsu K (2006) Development of wooden portal frame structures with improved columns. In: Proceedings 2006 World Conference on Timber Engineering, Oregon State Univ. Conference Services, Corvallis, OR, pp 311–318
9. Shim KB, Hwang KH, Park JS (2010) Lateral load resistance of hybrid wall. In: Proceedings 2010 world conference on timber engineering, Trees and Timber Institute, Sesto Fiorentino, Italy, pp 3166–3169
10. Hwang KH, Park JS, Shim KB (2010) Shear performance of hybrid post and beam wall system with structural insulation panel infill. In: Proceedings 2010 world conference on timber engineering, Trees and Timber Institute, Sesto Fiorentino, Italy, pp 3150–3157
11. Xiong HB, Liu YY, Yao Y, Li BY (2017) Experimental study on the lateral resistance of reinforced glued-laminated timber post and beam structures. J Asian Archit Build 16:379–385

12. Shu GP, Liu W, Chen SL (2014) Theoretical research on direct analysis method for semi-rigid steel frames (in Chinese). J Build Struct 35:142–150

13. Duan SJ, Wang R, Jin KH (2014) Analysis method for planar frames with generalized semi-rigid connections (in Chinese). J Shijiazhuang Tiedao Univ 27:1–7

14. Zonta D, Loss C, Piazza M, Zanon P (2011) Direct displacement-based design of glulam timber frame buildings. J Earthq Eng 15:491–510

15. Wang Y, Li HJ, Li JF (2003) INITIAL stiffness of semi-rigid beam-to-column connections and structural internal force analysis (in Chinese). Eng Mech 20:65–69

16. Xiong HB, Liu YY (2016) Experimental study of the lateral resistance of bolted glulam timber post and beam structural systems. J Struct Eng 142:E4014002

17. GB/T1231-2006 (2006) Specifications of high strength bolts with large hexagon head, large hexagon nuts, plain washers for steel structures (in Chinese). China Ministry of Construction, Beijing

18. GB 50017 – 2003 (2003) Code for design of steel structures (in Chinese). China Ministry of Construction, Beijing

19. ASTM E2126-11 (2011) Standard test methods for cyclic (reversed) load test for shear resistance of vertical elements of the lateral force resisting systems for buildings. American Society for Testing and Materials, West Conshohocken, p 8

20. He MJ, Zhao Y, Gao CY, Zhang JH (2015) Effect of bolt row and self-tapping screw reinforcement on lateral performance of bolted timber connection (in Chinese). J Tongji Univ 43:987–992

21. Krawinkler H, Parisi F, Ibarra L, Ayoub A, Medina R (2001) Development of a testing protocol for wood frame structures. Report W-02. CUREE-Caltech Woodframe Project, Stanford

22. Zhao Y (2016) Research on moment bearing performance and improvement methods of glulam multiple bolted connections in post-and-beam timber construction (in Chinese). PhD Thesis. College of Civil Engineering, Tongji University, Shanghai, China